Journal of Analytical and Applied Pyrolysis 162 (2022) 105457

Contents lists available at ScienceDirect

Journal of Analytical and Applied Pyrolysis

journal homepage: www.elsevier.com/locate/jaap

Pyrolysis kinetic, thermodynamic and product analysis of different leguminous biomasses by Kissinger-Akahira-Sunose and pyrolysis-gas chromatography-mass spectrometry

S. Clemente-Castro, A. Palma *, M. Ruiz-Montoya, I. Giráldez, M.J. Díaz

Pro2TecS–Product Technology and Chemical Processes Research Centre. Department of Chemical Engineering, Physical Chemistry and Materials Science. University of Huelva, Campus El Carmen, 21071 Huelva, Spain

ARTICLE INFO

Keywords:
Leguminous
Biofuel
Pyrolysis
KAS
Py-GC/MS

ABSTRACT

To ascertain the potential of various leguminous biomass such as *L. leucocephala*, *C. proliferus*, *P. alba* and *S. sesban*, both energetic and a source of high added value products, the pyrolytic behaviour was studied at different heating rates by using the analytical method of thermogravimetric (TG), isoconversional method of Kissinger-Akahira-Sunose (KAS), determination of some thermodynamic parameters and pyrolysis-gas chromatography-mass spectrometry (Py-GC/MS). It was concluded that biomass such as *L. leucocephala* or *C. proliferus* are more suitable for pyrolysis since less energy is required to degrade them, more evident in the final stages of degradation in which *P. alba* and *S. sesban* present very high activation energies calculated by KAS. All leguminous biomass produced volatile compounds with high phenol content at the peak of maximum degradation of hemicellulose, most of the heavy derivates are derived from lignin, such as ferulaldehyde or methoxyeugenol, because sufficient energy has not yet been provided to break down the structure. At this peak it can see some furans and saccharides in the case of *C. proliferus* since it has a higher C_5 content in its composition. A wide range of compounds were detected at the peak of maximum degradation of cellulose, *L. leucocephala* and *C. proliferus* produce more short-chain compounds that give rise to bio-oils whereas, *S. sesban* and especially *P. alba*, in addition, produce a quantity of high added value of saccharides such as levoglucosan and D-allose (4.73% and 13.94%, respectively).

1. Introduction

The rise in CO_2 levels in the atmosphere, which has increased by 42% since 1950, has resulted in climate change, a global issue. Industrial intensification and deforestation have made this sudden increase possible. Only by developing alternative energy sources not dependent on fossil resources and ensuring a balance in deforestation by safeguarding tropical forests, which are the great sinks of CO_2, will humanity manage to alleviate the negative effects of this global crisis [1]. Some of the alternative resources to replace fossil fuels and reduce the pollution they generate include solar, wind or hydroelectric energy, and biofuels [2].

Biofuels are generated from renewable sources such as agricultural residues, wood and herbaceous biomass, as well as other biological waste materials, which are renewed in relatively short time cycles [3,4]. In this sense, lignocellulosic biomass takes on special importance due to its large abundance, closed carbon cycle and conversion potential into a wide variety of high added value products for the chemical and energy industry [5]. Lignocellulosic biomass can be treated using different high-efficiency conversion technologies, such as pyrolysis, gasification, combustion and biochemical fermentation. In this sense, the thermochemical technologies mentioned above are already established processes for large-scale disposal of biomass waste, are well-established processes for the large-scale disposal, due to its easy of adaptation to current technologies in the fossil fuel industry [6]. Among other techniques, pyrolysis which operates in an inert atmosphere offers numerous advantages, including lower emissions and full utilization of by-products. In addition, these processes may be complementary and thus the design parameters of the equipment would be optimized knowing the different reaction mechanisms of each type of biomass more specifically [7].

Regarding the raw materials selected in this work, these are highly

* Corresponding author.
E-mail address: alberto.palma@diq.uhu.es (A. Palma).

https://doi.org/10.1016/j.jaap.2022.105457
Received 30 November 2021; Received in revised form 21 January 2022; Accepted 30 January 2022
Available online 2 February 2022

productive, fast-growing leguminous biomass with a series of characteristics that make them interesting, such as, for example, their suitable nitrogen fixation capacity. The studied biomass in this article are as follows: *Chamaecytisus proliferus*, a shrub native to the Canary Islands resistant to droughts, capable of controlling soil erosion and providing nutrients, which makes it popular as forage, will be studied [8]; *Leucaena leucocephala*, a tree with great energy potential and the ability to grow in relatively poor soils that adapts to dry and humid environments [9,10]; *Prosopis alba*, an arboreal species from South America and with good adaptation to dry and contaminated soils and, therefore, a good candidate for reforestation projects [11]; and *Sesbania sesban*, adaptable to the climatic and edaphic conditions of semi-arid and rocky areas, which have made it a popular species for fallow in parts of Africa by rehabilitating degraded soils [12]. Regarding its performance in thermochemical processes, pyrolysis has been studied for Tagasaste and Leucaena leucocephala at the University of Huelva, obtaining kinetic data from the raw material and, in the case of Leucaena, also applying pretreatments such as acid hydrolysis [10,13].

The mass loss behavior in thermochemical treatments is commonly determined by thermogravimetric analysis (TGA). TGA experiments with small samples and variable heating rates can result in a highly reliable kinetic regime with few limits on heat transfer and mass transport, this allows studying the conversion mechanisms by analysing the TGA curves [14]. The methods for the calculation of non-isothermal kinetic parameters can be divided into fitted model methods and isoconversional methods, each of which has its drawbacks and are used in a complementary way [15]. Isoconversional methods allow evaluating the evolution of the effective kinetic energy of the reaction without assuming a reaction model, which indicates a dependence on the degree of conversion that indirectly reflects the complexity of the reactions and mechanisms of the thermochemical treatments of biomass. There are numerous isoconversional kinetic methods including the Friedman differential method, the Ozawa-Flynn-Wall (FWO) integral method, the Kissinger-Akahira-Sunose (KAS) integral method, or the Vyazovkin nonlinear integral method [16,17].

Another aspect to consider in thermochemical treatments is the conversion of biomass to chemical products and fuels. Pyrolysis produces a mixture of gas, bio-oil, and char, which also is the initial step in gasification, therefore analyzing these products is critical for understanding the quality of the raw materials. Thermal desorption/gas chromatography-mass spectrometry (TD/GC-MS) is a technique that allows the analysis of small samples of volatile compounds and has been successfully applied to the pyrolysis of lignocellulosic biomass. Although this method is very useful, it has the disadvantage of resulting in a high number of compounds that overlap at the same retention time, making their treatment difficult, this is due to the complex lignocellulosic structure [18,19].

The goal of this research is to quantify the conversion characteristics of various leguminous biomass applying TGA by pyrolysis. *L. leucocephala*, *C. proliferus*, *P. alba* and *S. sesban* have been chosen, as high-yielding legume biomass, for this purpose. In addition, a study is carried out of the compounds generated during the pyrolytic degradation of leguminous biomass in the most distinctive points (hemicellulose and cellulose peak) by Py-GC/MS. With these data, interesting results and approaches are obtained to understand the behavior of the selected biomasses and their constituents in thermochemical treatments could be obtained. This data could aid the industry in the implementation of new equipment and processes as well as more sustainable production routes for high added value products.

2. Materials and methods

2.1. Feedstock preparation

The leguminous biomasses used in this study were *L. leucocephala*, *C. proliferus*, *P. alba*, and *S. sesban*, all of which are considered good candidates for reforestation and soil treatment due to their properties. *L. leucocephala* has multipurpose uses, such as firewood generation, timber, greens, fodder, and green manure, as well as to provide shade and control soil erosion [20], while *C. proliferus* has been used extensively as forage treeshrub [21], *P. alba* for the production of furniture and candidate for recovering degraded areas [22], and, finally, *S. sesban* has become popular as a fallow species in Africa [23]. All studied biomass has been collected from various plantations in Campus La Rábida, Huelva Universtiy (Huelva, Spain). These were stored wet and then air dried to reduce humidity to less than 10 wt% and followed by chipping down to pieces between 2 cm× 0,5 cm for further treatment. The pieces of woody, branches and twings that were used in the study were obtained by trimming the different plants, removing leaves and non-wood pieces before being crushed in a hammer mill (Retsch SM 2000) to a particle size of 0.5–5 mm in accordance with Tappi T-257 [24], which was the range chosen for all the experiments run on the thermogravimetric analyzer.

2.2. Biomass characterisation

The four leguminous biomasses were homogenized for elemental and proximate analyses. A Leco TruSpec CHN (University of Sevilla) and a Eltra Helios CHS (Universtiy of Huelva) were used to determine the elemental content of the samples, and for the proximate analysis with which were obtained moisture (M), volatile matter (VM), fixed carbon (FC) and ash content (AC) the ASTM D7582 method was followed using Mettler Toledo TGA/DSC1 STARe system [25].

The chemical component of biomass evaluated consists of ethanol-benzene extractives (TAPPI T-204) [26], Klason lignin and carbohydrates, mainly C_6 and C_5 sugars that represent well the fraction of cellulose and hemicellulose, respectively. For this purpose, each biomass was separated into portions of homogenized wood chips and subjected to acid hydrolysis with 72% sulphuric acid (TAPPI T-249) [27]. The solid residue recovered after acid hydrolysis and subsequently filtered is considered as the Klason lignin fraction. To obtain the content of acetic acid and monosaccharides found in hydrolisates, filtered samples were injected into the HPLC to determine the content of C_6 sugars (as glucan), C_5 sugars (as xylan and arabinan), and acetyl groups.

In addition to these data, gross heating values of the samples were determined according to CEN/TS standard 14918 (2005) and UNE standard 16001 EX (2005), using a Parr 6300 automatic isoperibol (bomb) calorimeter and 5.0 g of leguminous biomass pellets in each run.

2.3. Thermogravimetric analysis (TG)/derivate thermogravimetry (DTG) analysis of leguminous biomass

The thermogravimetric experiments were carried out by a thermogravimetric analyzer (TGA) (Mettler Toledo TGA/DSC1 STARe System). Thermogravimetric experiments were carried out for all samples in the decomposition range of 25 °C to about 800 °C under four heating rates of 5, 10, 15 and 20 °C min^{-1}. The initial mass of the samples used was around 10 mg. The TGA data were analyzed to determine the activation energy, E_a, using the isoconversional method described by Kissinger-Akahira-Sunose taking into account the assumption of Coats-Redfern. The inert gas used for the pyrolysis of leguminous biomass was 10 mL/min of nitrogen.

2.4. Analytic method (Kissinger-Akahira-Sunose). Activation energy calculation

The kinetics of chemical reactions in solids can be described by the rate of loss of the reactant, which is commonly determined as a derivation of the law of mass action, originally proposed by Guldberg and Waage [28]:

$$\frac{d\alpha}{dt} = k(T)f(\alpha), \tag{1}$$

where α is the conversion, t is the time, $d\alpha/dt$ is the rate of reaction, $k(T)$ is the rate coefficient at temperature T, and $f(\alpha)$ is a function of conversion, whose shape depends on the kinetic model.

The conversion of the sampling can be computed from the mass disappearance during the chemical reaction:

$$\alpha = 1 - \frac{m - m_f}{m_0 - m_f} = \frac{m_0 - m}{m_0 - m_f}, \tag{2}$$

where m is the mass of the sample remaining at time t, m_f is the final mass of the sample when the reaction is completed, and m_0 is the initial mass of the sample.

The reaction rate coefficient $k(T)$ is determined mostly by the equation of Arrhenius [29]:

$$k(T) = A\exp\left(-\frac{E_a}{RT}\right), \tag{3}$$

where A is the pre-exponential factor, E_a is the activation energy, and R is the universal constant of ideal gases ($8.3145JK^{-1}mol^{-1}$).

The rate of reaction taking the Arrhenius relation (3) can be expressed in differential form as can see in $Eq.(4)$:

$$\frac{d\alpha}{dt} = A\exp\left(-\frac{E_a}{RT}\right)f(\alpha) \tag{4}$$

When it operates under non-isothermal condition and temperature raises with time at a constant temperature ramp, $\beta = dT/dt$, $Eq.(4)$ can be represented as:

$$\frac{d\alpha}{dT} = \frac{A}{\beta}\exp\left(-\frac{E_a}{RT}\right)f(\alpha) \tag{5}$$

The integral form of the rate equation can be determined assuming the pre-exponential factor A do not depend on the temperature:

$$g(\alpha) = \int_0^\alpha \frac{d\alpha}{f(\alpha)} = \frac{A}{\beta}\int_{T_0}^{T} exp\left(-\frac{E_a}{RT}\right)dT \approx \frac{A}{\beta}\int_0^T exp\left(-\frac{E_a}{RT}\right)dT, \tag{6}$$

being the lower integration limit in the last integral approximately 0 since the rate of reaction is not significant for temperatures below initial temperature, T_0 [30].

The Kissinger-Akahira-Sunose (KAS) method corrected some deviations from simpler methods like Ozawa-Flynn-Wall, employing the approximation of Coats-Redfern [31]. The Arrhenius equation for KAS remains in the following expression:

$$Ln\left(\frac{\beta}{T^2}\right) = Ln\left(\frac{AR}{E_a g(\alpha)}\right) - \frac{E_a}{RT} \tag{7}$$

Representing graphically β/T^2 versus $1/T$ for constant conversion value gives a straight graph. Through the slope of this plot E_a value is obtained by multiplying this value by the universal constant of ideal gases, R.

2.5. 2.5. Thermodynamic parameters calculation

Once the activation energies have been calculated, the thermodynamic parameters can be determined through them, such as the pre-exponential factor (A) in Arrhenius equation, enthalpy (ΔH), free Gibbs energy (ΔG), and entropy (ΔS) which are obtained by the following equations [32,33]:

$$A = \beta \cdot E_a \cdot exp\left(\frac{E_a}{R\cdot T_m}\right) \Big/ \left(R\cdot T_m^2\right), \tag{8}$$

$$\Delta H = E_a - R\cdot T_\alpha, \tag{9}$$

$$\Delta G = E_a + R\cdot T_m \cdot Ln\left(\frac{K_B\cdot T_m}{h\cdot A}\right), \tag{10}$$

$$\Delta S = \frac{\Delta H - \Delta G}{T_m}, \tag{11}$$

where, T_m represents the peak temperature on the DTG graph, T_α the temperature at the given degree of conversion α, K_B Boltzmann constant ($1,381x10^{-23}JK^{-1}$) and h Plank constant ($6,626x10^{-34}J\ s$).

2.6. Volatile analysis by pyrolysis TD/GC-MS

Volatile compounds samples from the pyrolysis process in the maximum temperature ranges of *L. leucocephala*, *C. proliferus*, *P. alba*, and *S. sesban*, both the hemicelluloses and cellulose peaks, obtained at the exit of the TGA/DTG (heating rate: 20 K min^{-1}; N_2 flow: 20 cm^3 min^{-1}) were collected in fritted glass TD tubes (Supelco, Bellefonte, PA; O.D.: 6.35 mm; length: 88.9 mm) for 1.5 min. Tubes containing 100 mg of TenaxR TA (80–100 mesh purchased from Supelco, Bellefonte, PA) packed in layers of silanized glass wool. The experiments were replicated until the standard deviations of the data were < 5%.

TD tubes after sampling have been analyzed using TD/GC-MS. TD was used to release the captured volatile compounds from the tube sorbent material onto the GC/MS for identification and quantification. TD was carried out by use of thermal desorption system unit (TD-20, Shimadzu, Japan) fitted with a HP-5 MS column (60 m, 0.25 mm I.D. 0.25 µm film thickness, J&W Scientific, Agilent Technologies, USA) and involved 2 steps: tube desorption and trap desorption. In the tube desorption step TD tube was rapidly heated to 280 °C for 10 min to ensure complete desorption using helium (baseline 5.0, Afrox SA) as carrier gas at 10 mL/min and split flow of 40 mL/min (split ratio of 2.5). Released volatiles were then trapped into a general-purpose cold trap at − 16 °C. In the trap desorption stage, the cold trap was desorbed at 280 °C for 8 min and 1.3 mL/min helium flow through the transfer line to the GC-MS with 40 mL/min split flow. The transfer line was maintained at 280 °C to prevent volatile condensation. To avoid irreversible adsorption of the low volatile compounds by strong sorbent material in the TD tubes, the flow of carrier gas in both the tube and trap desorption stages was in the reverse direction, from the rear end to the sampling end of the TD tube/trap. A 3 min pre-purge of the system at 1 mL/min helium flow and room temperature was done before each analysis to reduce oxygen and/or moisture in the system.

The mass spectrometer was operated in scan mode (41–450 m z^{-1}). Volatile organic compounds were identified by comparison of the mass spectra with those in the database of NIST11 library using as internal standard 1-bromo-3-chlorobenzene. For control and data analysis, the GCMS Postrun Analysis Shimadzu was used. The MS was turned with perfluorotributylamine (PFTBA).

3. Results and discussion

The chemical compositions, as well as their properties and elemental analysis of leguminous biomass are available in Table 1. After three replications of each sample, the moistures obtained were 7.03, 5.86, 7.74 and 7.15 for *L. leucocephala*, *C. proliferus*, *P. alba* and *S. sesban*, respectively. *L. leucocephala*, *P. alba* and *S. sesban* showed the highest volatile matter (VM) compared to the *C. proliferus* which is a non-woody shrub biomass. The low percentages of ash in these woody samples are in agreement with the bibliography of woody biomass (≤3%wt) [34]. *L. leucocephala* has a higher content of C_6 sugars and lignin related to its chemical composition, the other biomasses have more discrete values of these parameters. The relative high content of C_6 sugars in *L. leucocephala* and *P. alba*, but especially in *S. sesban* (50,9% wt.), can be explained by the range of cellulose content 40–46% [35,36] and hemicellulose present to a large extent as glucomannan. Contents as high in

Table 1
Characteristic properties of leguminous biomass feedstocks.

Property	Feedstock			
	L. leucocephala	*C. proliferus*	*P. alba*	*S. sesban*
Proximate analysis (wt%), db[a]				
Volatile matter (VM)	81.67	58.25	78.44	82.30
Ash content (AC)	1.99	23.32	3.34	2.04
Fixed carbon (FC)	16.34	18.43	18.22	14.54
Ultimate analysis (wt%), daf[b]				
C	47.30	46.10	41.33	46.58
H	6.05	4.51	4.75	5.35
N	1.90	2.00	0.58	1.21
S	0.02	0.01	0.01	0.01
O[c]	41.60	45.30	48.20	41.18
Lignocellulose composition (wt%), daf[b]				
Klason lignin	22.7	19.7	19.2	26.2
Extractives	1.9	2.3	4.7	2.6
C_6 sugars	37.1	39.3	41.6	50.9
C_5 sugars	18.4	21.2	17.8	16.4
Acetyl groups	2.1	4.4	3.3	3.1
Gross heating value over dry basic				
GHV, MJ/kg	18.8	19.4	18.1	18.9

[a] Dry basis.
[b] Dry ash free basis.
[c] Determined by difference.

lignin as those shown by *L. leucocephala*, *P. alba* and *S. sesban* were characteristic of softwoods, with previously reported values for this species of between 20% and 28% wt. [37,38], but, in reality, all leguminous biomass are hardwood species with lignin content that varies and determine its characteristics.

C. proliferus is a non-woody tree-shrub legume biomass, and the fundamental component of hemicellulose is xylan [39], the content of C_5 and C_6 sugars is expected to be similar to hemicellulose and cellulose, respectively. In studies for the valorization of *C. proliferus* to obtain sugars and good quality of its pulp to produce paper [13,37], chemical compositions in ranges of 18–24%, 35–45% and 17–25% for hemicellulose, cellulose and lignin contents, respectively, have been reported results that conform to those obtained in this article. Compared with the other leguminous species, *C. proliferus* was the one with the highest content of C_5 sugars, that is, hemicellulose (Table 1). Unusually, the high ash content of *C. proliferus* (23,3% wt. in basis dry) might be attributed to its mineral absorption capacity of this specie and to the soil conditions during sample harvesting. As can be seen, *S. sesban* was the biomass with the highest lignin content, a key component in the formation of char and FC, however it obtained the lowest FC content, therefore, the other polymers in biomass (hemicellulose and cellulose) present a contribution to FC content. The nature of different lignins and their thermal stabilities may also be the reason, since some biomass show distributions of guaiacyl (G) and syringyl (S) units with variable amounts of *p*-hydroxyphenyl (H) units, while others G clearly dominate [40].

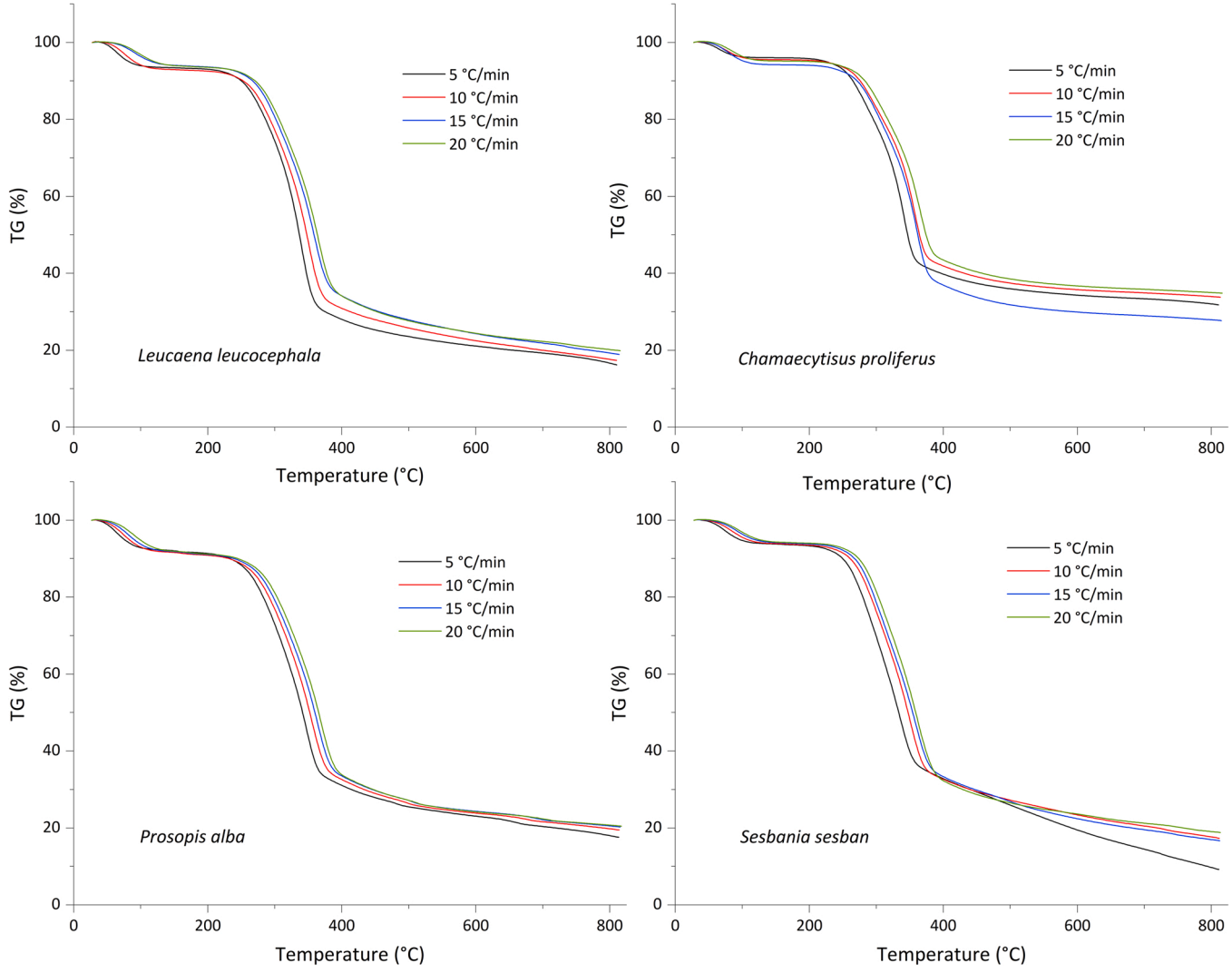

Fig. 1. Thermogravimetry (TG) analysis of different leguminous biomass at different heating rates.

3.1. Thermogravimetric characteristics analysis of leguminous biomass

3.1.1. Thermogravimetry (TG) analysis

The thermogravimetric curves of leguminous biomass *L. leucocephala*, *C. proliferus*, *P. alba* y *S. sesban* are shown in Fig. 1. As can be seen in the graphs, when the heating rates are increased, an escalation in the temperature at which the reactions take place is observed in the curves. This effect is very similar in all leguminous biomass samples. Although it has small variations, for a conversion rate of 0.5, the pyrolysis temperatures of samples at the heating rate of 5, 10, 15, and 20 °C min^{-1} were 327 °C, 337 °C, 343 °C, and 348 °C subsequently.

Furthermore, when the reaction of volatiles was at a conversion rate between 0.1 and 0.9, the main pyrolysis temperature intervals of *L. leucocephala*, *C. proliferus*, *P. alba*, and *S. sesban* were 235–494 °C, 248–432 °C, 233–474 °C and 244–490 °C, respectively. The temperature at which the reaction is completed in *C. proliferus*, taken as 0.9 of conversion, is significantly lower than the other leguminous, possibly due to the high percentage of ash content from this that would be acting as a catalyst. The variable amount of ash in *C. proliferus* samples made the end of the thermogravimetric curves inconsistent, in addition the conditions of the experience with *S. sesban* at 10 °C min^{-1} led to a prolonged loss of the almost total fixed carbon fraction with no effect in subsequent activation energy calculations. However, it was observed that the starting temperature of the reactions is slightly lower in the case of *P. alba* and consequently the start of pyrolysis occurs earlier compared with the other samples. In the biomass pyrolysis process, three reaction steps were reported: dehydration, devolatilization and decomposition of solids, for wood biomass such as *Pinyon pine*, whose devolatilization range was 210–400 °C [41] or recent thermogravimetric studies of our leguminous, *L. leucocephala* [10] and *C. proliferus* [13], with devolatilization ranges between 235 and 475 °C and 255–435 °C. These results are consistent with data obtained in this study.

3.1.2. Derivative thermogravimetric (DTG) analysis

The DTG curves of the four leguminous biomasses are shown in Fig. 2. The behavior of the DTG curve in the main pyrolysis zone (200–400 °C) is divided in two, showing two specific peaks in the case of *S. sesban* and two stages without differentiating peaks but trends are observed with their respective more prominent inflection points in the case of *L. leucocephala* and *C. proliferus*, and slightly diffuse in *P. alba*. This could be due to the different structure and composition between different biomasses that indicate changes in the simultaneous degradation mechanisms in hemicellulose and cellulose [42].

Regarding the increase in heating rate, the reaction rate rose for all samples as clearly seen in the DTG curves. For heating rate of 20 °C min^{-1}, the maximum reaction rate of *C. proliferus* (23.56% min^{-1} at 367 °C) is the highest of all probably due to the elevated ash content that partially catalyses the reaction and its shrub condition that makes it more susceptible to thermochemical treatments, followed by *L. leucocephala* (19.90% min^{-1} at 364 °C), *P. alba* (18,01% min^{-1} at

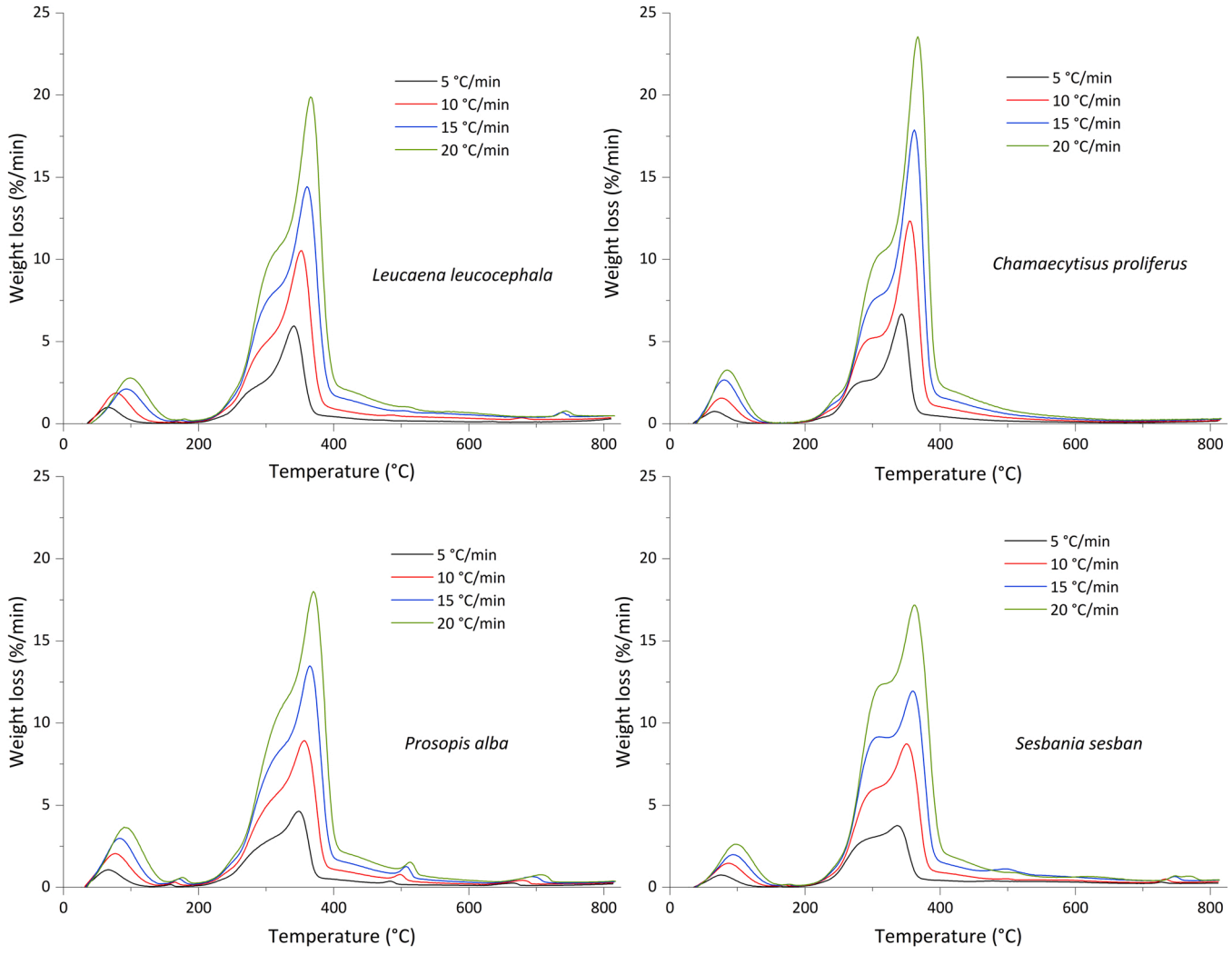

Fig. 2. Derivative thermogravimetry (DTG) analysis of different leguminous biomass at different heating rates.

370 °C) and finally *S. sesban* (17.18% min^{-1} at 367 °C) with the lowest value. In the case of slower pyrolysis (5 °C min^{-1}), the biomass decomposes with the same pattern being the fastest *C. proliferus* (6,68% min^{-1} at 343 °C), followed by *L. leucocephala* (5.95% min^{-1} at 339 °C), *P. alba* (4.64% min^{-1} at 348 °C) and finally *S. sesban* (3.76% min^{-1} at 337 °C). Besides, the degradation peaks of hemicelluloses understood as points of trend change in the DTG curves, the disposition of reaction rates are inverse to the cellulose peak, since the reactions are complementary, and the connections would be tighter in the structure of the two components. On this occasion, *S. sesban* had the highest hemicellulose reaction rate (12.28% min^{-1} at 310 °C), followed by *P. alba* (11.14% min^{-1} at 325 °C), and finally with similar reaction rates *C. proliferus* and *L. leucocephala* (9.63% min^{-1} and 9.53% min^{-1}, respectively, at 300 °C for both of its). These data show that in pyrolysis treatments of leguminous, higher heating rates offer better reaction rates, therefore, it is preferable to perform at the highest possible heating rate.

3.1.3. Pyrolysis kinetics analysis with Kissinger-Akahira-Sunose energy model (KAS method)

The data from the kinetic analysis for the different leguminous biomass are shown in Table 2 and Fig. 3, where a graph of the evolution of the activation energies with respect to the degree of conversion of each sample (α in the range of 0.05 and 0.90). Activation energies were calculated using the KAS isoconversional method for heating rates of 5, 10, 15 and 20 °C min^{-1}.

The evolution of the activation energy in all the biomasses studied clearly shows that the pyrolysis of lignocellulosic materials is not a single-stage reaction but rather a highly complex multi-stage reaction in which each reaction contributes in part to the global mechanism. With increasing degree of conversion, pyrolysis can be approximately separated in three stages that assimilated with the different conversion zones in the TG/DTG curves, except for the first dehydration phase in which it is observed that the activation energy drops drastically by losing 10% of the average amount of water per sample. Stage I, stage II and stage III, take place in a conversion range of 0.15–0.35, 0.35–0.55 and 0.55–0.90, corresponding to temperatures of 120–300, 300–330, and 330–800 °C, respectively. In stage I, the activation energy values tend to increase, as in the case of *L. leucocephala* from 159.84 kJ mol^{-1} to 205.20 kJ mol^{-1} or stabilize around average values, *C. proliferus* from 183.46 kJ mol^{-1} to 185.11 kJ mol^{-1} and *S. sesban* from 178.01 kJ mol^{-1} to 169.98 kJ mol^{-1}, only *P. alba* suffered a fall from 214.51 kJ mol^{-1} to 183.05 kJ mol^{-1} following a trend towards stability around

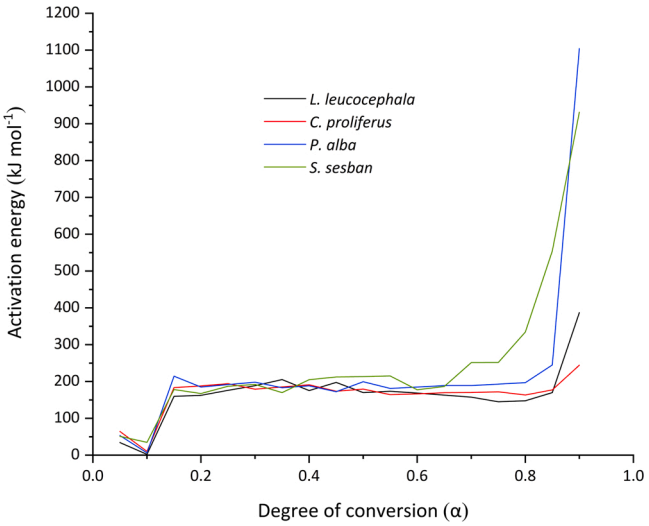

Fig. 3. Changes of the activation energies during the pyrolysis of different leguminous biomasses derived from Kissinger-Sunose-Akahira method.

190 kJ mol^{-1} after the strong rise after dehydrating due to the more timber structure possibly. With reference to TG/DTG analysis in Fig. 1 and recent reports [17], most hemicelluloses and extractives degrade at this stage, while other shorter chain compounds such as fats, protein and ammonium are easily lost at lower temperatures hence the low initial activation energies. In stage II, the activation energies clearly stabilize around a specific value, it is the main stage of decomposition of celluloses. In this study, the average activation energies of leguminous at this stage are: 183.75 kJ mol^{-1}, 178.45 kJ mol^{-1}, 184.70 kJ mol^{-1} and 202.25 kJ mol^{-1}, to *L. leucocephala*, *C. proliferus*, *P. alba* and *S. sesban*, respectively. These results are consistent with previous studies of cellulose compounds, thus Lin et al. [43], obtaining a value of 198 kJ mol^{-1} for pure cellulose, Sánchez-Jiménez et al. [44] which explored the kinetics of cellulose thermal degradation under a combined isoconversional and generalized master plot approach resulting 191 kJ mol^{-1} and Bhagwan Dahiya et al. [45] obtaining a value of 166.5 kJ mol^{-1} studying isothermal and non-isothermal degradation processes. In the stage III, the activation energies were significantly increased, although roughly among leguminous. While the leguminous samples with more robust wooden structures, the evolution of the activation energies is very fast, as in case of *P. alba* and *S. sesban* that scale

Table 2
Activation energy of leguminous biomass at different conversion rate α calculated by using the Kissinger-Akahira-Sunose (KAS) method based on different heating rates (5 °C min^{-1}, 10 °C min^{-1}, 15 °C min^{-1}, 20 °C min^{-1}).

Degree of conversion (α)	*L. leucocephala*		*C. proliferus*		*P. alba*		*S. sesban*	
	E_a (kJ mol^{-1})	R^2	E_a (kJ mol^{-1})	R^2	E_a (kJ mol^{-1})	R^2	E_a (kJ mol^{-1})	R^2
0.05	34.03	0.973	64.45	0.991	53.08	0.980	51.07	0.999
0.10	2.22	0.232	10.24	0.503	6.28	0.244	34.83	0.490
0.15	159.84	0.946	183.46	0.953	214.51	0.905	178.01	0.990
0.20	162.52	0.943	188.11	0.990	184.79	0.987	167.42	0.979
0.25	175.92	0.986	194.12	0.990	191.80	0.987	187.12	0.989
0.30	188.53	0.984	179.05	0.998	198.13	0.987	192.10	0.989
0.35	205.20	0.963	185.11	0.967	183.05	0.996	169.98	0.680
0.40	175.49	0.978	190.98	0.998	188.27	0.996	204.85	0.989
0.45	197.46	0.987	173.55	0.996	172.28	0.995	212.40	0.989
0.50	169.78	0.993	179.52	0.997	199.33	0.996	213.10	0.996
0.55	173.42	0.994	164.31	1.000	181.14	0.995	215.05	0.986
0.60	168.58	0.986	166.54	1.000	185.03	0.995	177.58	0.992
0.65	162.97	0.999	169.51	0.991	188.84	0.995	186.56	0.967
0.70	157.64	0.992	170.23	1.000	188.84	0.995	251.34	0.969
0.75	144.80	0.984	171.91	0.991	192.83	0.995	251.61	0.323
0.80	147.59	0.984	163.47	0.991	196.88	0.995	334.58	0.801
0.85	169.78	0.920	177.20	1.000	244.96	0.988	554.60	0.832
0.90	387.13	0.763	244.16	0.989	1103.93	1.000	931.35	0.792

up to 1103.93 kJ mol^{-1} and 554.60 kJ mol^{-1} to 0.9 of conversion rate; *L. leucocephala* was not so abrupt, only up to 387.13 kJ mol^{-1}; and *C. proliferus* followed an upward trend but much smoother until reaching a value of 244.16 kJ mol^{-1}. The activation energy is the strength that has to be overcome for the reaction to begin to occur, therefore the higher the value, the more difficult the process experiences to carry out. This stage III refers principally to the pyrolysis of the fraction associated with lignin, it is a much more complex thermochemical process, some authors suggested that it is a process in several stages with two, three or even four stages, whose reaction mechanism is uncertain due to its recalcitrant structure [46,47]. It is clear that the minerals remaining in the leguminous biomass samples in these last stages act as a barrier to the diffusion of heat and the release of long-chain volatile compounds, greatly increasing the activation energy. Nonetheless, in the case of biomass of a less woody character, lower activation energy values were obtained, even resulting in a slight rise such as *C. proliferus* in spite of an excessive amount of minerals in the form of ash, most likely due to a shrubby structure more tolerant to reaction and partially catalyzed. In fact, the lignin itself does not have a high activation energy but rather moves in values of around 175 kJ mol^{-1} [48].

In any case, it is well known that the pyrolytic processes of decomposition of lignocellulosic biomass do not occur in series otherwise that they occur simultaneously with each other and are far from independent [49]. Although these processes are difficult to know exactly, it is possible to see areas in which their main compounds are clearly decomposed. Therefore, the activation obtained in each zone should be considered as apparent activation energies of hemicellulose, cellulose and lignin compounds.

3.2. Thermodynamic analysis

The thermodynamic parameters of A, ΔH, ΔG, and ΔS of leguminous samples were calculated using as reference the activation energies obtained by the Kissinger-Akahira-Sunose method. The experimental values of the runs with lower heating rate were taken, which have the lowest interactions between constituents that increase with the rise in the heating rate reducing the effects of that reduction, therefore, for calculations data of 5 °C min^{-1} was chosen. The thermodynamic parameters are collected in Table 3, Table 4, Table 5 and Table 6, in the case of *L. leucocephala*, *C. proliferus*, *P. alba* and *S. sesban*, respectively.

The value of the pre-exponential (A) alters from on leguminous species to another, although in all of them it evolves upwards to high values, which indicates a complex composition that develops with increasing temperature. Woodier leguminous biomass such as *P. alba* and *S. sesban*, range from low values ($4.54 \cdot 10^{-3}$ s^{-1} and $7.22 \cdot 10^{2}$ s^{-1}) to very high values of the order of 10^{35} and 10^{84}, respectively. On the other hand, *L. leucocephala*, with a moderate woody structure, and *C. proliferus*, a shrub biomass, only rose from $4.27 \cdot 10^{-4}$ s^{-1} and $3.16 \cdot 10^{-2}$ s^{-1}, to $2.14 \cdot 10^{24}$ s^{-1} and $1.46 \cdot 10^{25}$ s^{-1}. Values of the pre-exponential factor less than 10^{-4} are related to lower activation energies and represent the degradation stages of hemicelluloses. These values indicate a faster and easier degradation effect of these biomass fractions for the respective degrees of conversion [50]. With the increase in the degree of conversion associated with the decomposition range of cellulose and lignin components (conversion between 0.35 and 0.85), the values of A are more than 10^{14} which indicates slow and complex degradation effects that require a greater number of molecular collisions to occur [51]. High values of A would require a higher activation energy, which is in agreement with the data in Table 1 in the later stages of the reaction.

Table 3
Thermodynamic parameters during the pyrolysis process of L. leucocephala under the heating rate of 5 °C.

Leucaena leucocephala				
Degree of conversion (α)	*A (s^{-1})*	*ΔH (kJ mol^{-1})*	*ΔG (kJ mol^{-1})*	*ΔS (J mol^{-1})*
0.10	4.27×10^{-4}	*-2.01*	*107.48*	*-323.00*
0.25	1.96×10^{25}	*171.23*	*95.17*	*224.39*
0.40	1.68×10^{25}	*170.59*	*95.17*	*222.47*
0.55	7.97×10^{24}	*168.39*	*95.21*	*215.87*
0.70	2.68×10^{22}	*152.50*	*95.47*	*168.22*
0.85	2.14×10^{24}	*164.27*	*95.27*	*203.55*

Table 4
Thermodynamic parameters during the pyrolysis process of C. proliferus under the heating rate of 5 °C.

Chamaecytisus proliferus				
Degree of conversion (α)	*A (s^{-1})*	*ΔH (kJ mol^{-1})*	*ΔG (kJ mol^{-1})*	*ΔS (J mol^{-1})*
0.10	3.16×10^{-2}	*5.89*	*104.50*	*-287.48*
0.25	6.01×10^{27}	*189.54*	*96.11*	*272.38*
0.40	1.97×10^{27}	*186.16*	*96.15*	*262.42*
0.55	1.47×10^{23}	*159.31*	*96.58*	*182.88*
0.70	1.22×10^{24}	*165.12*	*96.48*	*200.12*
0.85	1.46×10^{25}	*171.86*	*96.37*	*220.09*

Table 5
Thermodynamic parameters during the pyrolysis process of P. alba under the heating rate of 5 °C.

Prosopis alba				
Degree of conversion (α)	*A (s^{-1})*	*ΔH (kJ mol^{-1})*	*ΔG (kJ mol^{-1})*	*ΔS (J mol^{-1})*
0.10	4.54×10^{-3}	*2.66*	*107.56*	*-301.45*
0.25	9.76×10^{26}	*187.27*	*97.67*	*257.46*
0.40	2.82×10^{26}	*183.47*	*97.72*	*246.41*
0.55	2.32×10^{25}	*176.15*	*97.83*	*225.03*
0.70	3.46×10^{26}	*183.69*	*97.71*	*247.07*
0.85	1.19×10^{35}	*239.23*	*96.96*	*408.83*

Table 6
Thermodynamic parameters during the pyrolysis process of S. sesban under the heating rate of 5 °C.

Sesbania sesban				
Degree of conversion (α)	*A (s^{-1})*	*ΔH (kJ mol^{-1})*	*ΔG (kJ mol^{-1})*	*ΔS (J mol^{-1})*
0.10	7.22×10^{2}	*30.53*	*99.27*	*-203.99*
0.25	1.56×10^{27}	*182.56*	*94.56*	*261.13*
0.40	9.54×10^{29}	*200.06*	*94.31*	*313.81*
0.55	3.82×10^{31}	*210.06*	*94.17*	*343.88*
0.70	1.89×10^{37}	*246.18*	*93.73*	*452.37*
0.85	4.20×10^{84}	*547.77*	*91.52*	*1353.87*

The enthalpy change (ΔH) is a measure of the energy differences between the activated complex and the reactants [52]. As shown in the tables of thermodynamic parameters, enthalpies increase to stable values during cellulose degradation and finally rise with the arrival of the predominance of lignin degradation, which are more evident in the case of *P. alba* and *S. sesban*. The average values of cellulose are 165 kJ mol^{-1}, 174 kJ mol^{-1}, 182 kJ mol^{-1} and 208 kJ mol^{-1} for *L. leucocephala*, *C. proliferus*, *P. alba* and *S. sesban*, respectively. The results show that a higher content of lignin composition in its composition requires more energy to break the bonds, for example, *S. sesban* with a high Klason lignin content (26.2%) had 547.77 kJ mol^{-1} for a degree of conversion located in the last stages of degradation.

The changes of the Gibbs free energy (ΔG) describe the total energy of the system at the point where the reactants become active complex [51,53]. During the degradation of the different leguminous biomass no significant changes are observed in the ΔG except at the beginning of the degradation of hemicelluloses where a higher value is appreciated, since

at that point the temperature is not yet high enough and the active complex needs a little more energy to form.

Entropy (ΔS) is the thermodynamic parameter that represents the degree of disorder of the reaction as a function of state. Low values of entropy mean that the reaction system must go through some type of physical or chemical step to reach equilibrium, while large values indicate that the equilibrium has already been exceeded and the reactivity of the system is high, producing the active complex easily and giving low reaction times [33,51,53]. The data shows that at sufficient temperatures (>300 °C) which cellulose and lignin reactions dominate, sufficient quantity of heat is available to form the active complex and the reaction is spontaneous.

3.3. Pyrolysis-gas chromatography-mass spectrometry (Py-GC/MS) analysis of leguminous biomass

One of the most important aspects to quantifying volatile compounds by thermal desorption is the selection of a suitable sorbent material. The material must be capable of collecting the most essential compounds to understand the thermal degradation process of samples and, in addition, that these are adequately desorbed in the heating/desorption equipment that is carried out with a reverse gas flow. Biomass is a complex structure that results in a wide variety of compounds with a wide spectrum of volatility. Although a multiple adsorbent would be adequate, a system with a single sorbent type Tenax Ta is implemented. Tenax Ta is made of a porous polymer, and which is a strong sorbent useful for compounds of a range of n-C_5-n-C_{30}.

Pyrolysis products of *L. leucocephala*, *C. proliferus*, *P. alba* and *S. sesban* detected by Py-GC/MS are shown in Table 7, additionally, Fig. 4 shows an example of a pyrogram, in this case associated with the hemicelluloses peak in pyrolysis degradation of *S. sesban*. Significant differences were observed between the different leguminous species and their respective hemicellulose and cellulose degradation peaks.

3.3.1. Py-GC/MS analysis at hemicellulose peak

For the degradation peak of hemicelluloses, which is around 300 °C, a very coincident amount of short-chain compounds is observed in all leguminous species, perhaps a little higher in the case of *C. proliferus* (19.12% instead of 16.89. 16.78. and 16.58% in case of *L. leucocephala*, *P. alba* and *S. sesban*. respectively) due to its condition as a shrub already mentioned, which makes it more vulnerable to thermochemical treatments. Acetyl substitutes for hemicelluloses are known to be a relevant source of acetic acid production during pyrolysis [54], therefore, its quantification is usually an indicator of acetyl groups, as can be seen, the only one that captures acetic acid is *C. proliferus*, which is associated with its superior content of acetyl groups that can be seen in Table 1. Some compounds stand out such as 2-hydroperoxyheptane in *L. leucocephala* ($C_7H_{16}O_2$. 5.76%) and *S. sesban* ($C_7H_{16}O_2$, 3.75%), ketones such as 1-hydroxypropan-2-one in the case of *C. proliferus* ($C_3H_6O_2$, 5.15%) and *P. alba* ($C_3H_6O_2$, 4.56%) or diethoxymethyl acetate ($C_7H_{14}O_4$) with influence on all of them. Another compound that is important in this peak is glutaraldehyde, a powerful cross-linking agent [55], which accounts for up to 9.62% to *P. alba*.

Regarding nitrogenous compounds, the only one that is significantly detected is sec-butyl nitrite with 6.76%, 2.13% and 7.01% in *L. leucocephala*, *P. alba* and *S. sesban*, respectively; not being detected in the *C. proliferus* where it breaks more easily. Furans, another interesting compound for the degradation of hemicelluloses and cellulose, were beginning to be obtained to a small extent in *C. proliferus* and *P. alba* in the form of furfural ($C_5H_4O_2$, 1.12% and 1.51%, respectively), the higher content of C_5 sugars in the form of xylan of the *C. proliferus* (Table 1) could be the cause of starting to detect furfural in the first degradation peak of the biomass [56]. The measurements of saccharides were not appreciable except in biomass with woodier characteristics with special attention to *P. alba* that already at this peak shows a quantity of 1,4:3,6-dianhydro-α-D-glucopyranose ($C_6H_8O_4$, 1.72%) and 3,4-altrosan ($C_6H_{10}O_5$, 2.02%).

With respect to the lignin derivates, it can be seen that these are the compounds that have been retained to greater extent. These very high amounts of phenol-derived compounds (G, S and L units) in the volatile fraction from pyrolysis indicate that the groups remain intact, with hardly any secondary reactions typical of higher heating rates that substitute methyl groups for methoxy groups [57]. Lignin from hardwood (mostly composed of G and S units), typically counts with larger methoxy groups than in softwood (mostly composed of G units), though non-woody lignin like wheat straw has intermediate values [58]. In these early stages of degradation it is observed that the S units attract attention enormously, with much importance of the syringol itself and methoxyeugenol, while G units are found to a lesser extent, being dominated by more complex and heavier guaiacols like 3-(4-hydroxy-3-methoxyphenyl)prop-2-enal (Ferulaldehyde) in the case of *L. leucocephala* and *S. sesban*, or 1-(4-hydroxy-3-methoxyphenyl)propan-2-one (Guaiacylacetone) in the case of *C. proliferus* and *P. alba*. As for L units, 1-(3,5-dimethoxyphenyl)ethanone clearly appears as the main compound from pyrolysis of our leguminous species. Therefore, at the hemicelluloses peak, the necessary interaction has not yet occurred to break the cellulose and lignin structure properly. Some other aromatic and heavy compounds were also formed in all species as a result of the degradation of extractives and other reactions.

3.3.2. Py-GC/MS analysis at cellulose peak

When leguminous biomasses were pyrolyzed at 360 °C approximately, the captured compounds showed a different behavior due to the decomposition of cellulose and a greater impact on lignin compared to the other compounds at 300 °C by increasing the reactivity of the system. The amount and variety of short-chain compounds derived from carbohydrates and phenols was significantly increased, especially in the case of *C. proliferus* in which up to 11 different compounds can be observed. Ketones can be highlighted as 1-hydroxypropan-2-one in the case of *L. leucocephala* ($C_3H_6O_2$, 5.13%), 3-Methyl-3-buten-2-one in the case of *P. alba* (C_5H_8O, 10.17%) or 3-methylcyclopentane-1,2-dione and 2-hydroxycyclopent-2-en-1-one in the case of *C. proliferus* ($C_6H_8O_2$, 4.66% and $C_5H_6O_2$, 3.33%, respectively), on the other hand, for *S. sesban*, compounds such as methyl isopropyl carbonate ($C_6H_{12}O_3$, 3.43%) are more important. These compounds are formed from the breakdown of sugar rings, mostly carbohydrates, in biomass [59]. For the maximum degradation of hemicellulose, high concentrations of glutaraldehyde were reached in all leguminous species with 13. 7.56. 5.92% and 8.54% in the case of *L. leucocephala*, *C. proliferus*, *P. alba* and *S. sesban*, respectively.

The decrease in sec-butyl nitrite is due to the increase in reactivity that destroys it to lighter compounds that were not detected, although if it resists the conditions in the case of *S. sesban* ($C_4H_9NO_2$.,7.85%). Furan compounds are dehydration products of carbohydrates and are formed in small amounts during pyrolysis [60]. In this research, the concentration of furans increases in cellulose peak mainly due to the total destruction of C_5 sugars and dehydration of some C_6 sugars, furfural grows in *C. proliferus* and *P. alba* up to 2.88% and 2.66% ($C_5H_4O_2$), respectively; 2,5-dimethylfuran ranks as the main furan compound in *L. leucocephala* (C_6H_8O, 0.82%) also appearing in moderate concentration in *P. alba* (C_6H_8O, 3.85%) and *C. proliferus* presents 2 H-furan-5-one ($C_4H_4O_2$, 2.94%) up to a total of 8.03% furan content, the highest in conjunction with *P. alba* with 6.51%. No furan was observed in the gas samples from the *S. sesban* pyrolysis process, this is due to the lower C_5 content that we can see in Table 1, since furans contain 5 atoms of carbon obtained mostly by the conversion of a polymer constituted by a framework of pentoses [61].

Anhydrosugars and furans are products obtained from depolymerization of hemicelluloses and cellulose by breaking β-1,4-glycosidic bonds between monomer units followed by intramolecular rearrangement of its [6,61]. The amount of volatile sugars that are detected in the maximum degradation peak of cellulose is very remarkable.

Table 7
Pyrolysis-gas chromatography-mass spectrometry (Py-GC/MS) products of leguminous biomass at different degradation peak.

Compound name	L. leucocephala		C. proliferus		P. alba		S. sesban	
	300 °C	365 °C	300 °C	365 °C	325 °C	360 °C	305 °C	360 °C
Carbohydrates-derived/ short chain compounds								
Acetic acid	–	–	1.95	1.03	–	–	–	–
2-hydroperoxyheptane	5.76	0.69	–	–	0.00	6.73	3.75	1.42
Pentane-1,2,3,4-tetrol	1.69	0.00	–	–	–	–	1.14	0.00
1-hydroxypropan-2-one	0.00	5.13	5.15	0.00	4.46	0.00	–	–
3-methylbutanal	–	–	–	–	0.97	0.00	0.00	2.72
3-Methyl-3-buten-2-one	–	–	–	–	0.00	10.17	–	–
methyl 3-hydroxypropanoate	–	–	0.00	1.44	–	–	–	–
2,3-dihydroxypropanal (Glyceraldehyde)	1.03	0.00	–	–	0.41	0.00	–	–
3-methylhexa-2,4-diene	–	–	–	–	0.00	4.20	–	–
Propane-1,2,3-triol (Glycerin)	–	–	1.87	0.00	–	–	–	–
Diethoxymethyl acetate	2.25	1.40	2.73	2.72	1.25	2.35	2.26	1.47
Methyl isopropyl carbonate	5.09	0.00	–	–	–	–	3.03	3.43
1-Acetoxy-propan-2-one	–	–	0.00	1.97	–	–	–	–
1,1-dimethoxypropan-2-one	–	–	1.77	1.10	–	–	–	–
4-hydroxybutanoic acid	–	–	0.00	0.84	–	–	–	–
3-methylcyclopentane-1,2-dione	0.00	1.72	0.00	4.66	–	–	–	–
Butyl isobutyl carbonate	1.07	0.00	–	–	–	–	–	–
2-hydroxycyclopent-2-en-1-one	–	–	0.00	3.33	–	–	–	–
Pentanedial (Glutaraldehyde)	0.00	13.00	5.65	7.56	9.62	5.92	6.40	8.54
3-Ethyl-2-hydroxy-2-cyclopenten-1-one	0.00	0.72	0.00	1.89	–	–	–	–
2-Propenyl butanoate (Butyric acid)	0.00	8.27	–	–	–	–	0.00	2.35
3-methyl-6-oxo-2-hexenyl acetate	–	–	0.00	1.00	–	–	–	–
Sub-total	16.89	30.93	19.12	27.54	16.71	29.37	16.58	19.93
Nitrogen compounds								
sec-Butyl nitrite	6.76	2.47	–	–	2.13	0.00	7.01	7.85
Furans compounds								
2,5-dimethylfuran	0.00	0.82	–	–	0.00	3.85	–	–
Furan-2-carbaldehyde (Furfural)	–	–	1.12	2.88	1.51	2.66	–	–
Furan-2-ylmethanol (Furfuryl alcohol)	0.00	0.09	0.00	2.21	–	–	–	–
2 H-furan-5-one	–	–	0.00	2.94	–	–	–	–
Sub-total	0.00	0.91	1.12	8.03	1.51	6.51	–	–
Saccharides compounds								
Bicyclo[2,2,2]octane-1,4-diol	0.00	0.19	0.00	0.29	–	–	–	–
1,4:3,6-Dianhydro-α-D-glucopyranose	0.00	2.22	0.00	1.66	1.72	2.56	–	–
3,4-Anhydro-D-galactosan	0.00	0.44	–	–	0.41	0.57	0.00	1.68
2,3-Anhydro-D-mannosan	0.00	0.71	–	–	0.00	1.00	0.00	0.35
2,3-Anhydro-D-galactosan	0.00	1.54	–	–	–	–	0.00	0.44
1,6-Anhydro-β-D-glucopyranose (Levoglucosan)	–	–	–	–	0.00	4.73	0.00	1.32
3,4-Altrosan	–	–	0.00	2.91	2.02	8.68	0.37	3.16
D-Allose	–	–	0.00	4.99	0.46	13.94	0.49	6.89
Sub-total	0.00	5.10	0.00	9.85	4.61	31.48	0.86	13.84
Lignin-derived compounds								
Guaiacol units (G)								
2-methoxyphenol (Guaiacol)	0.00	1.85	0.83	2.20	1.07	1.54	1.21	1.44
2-methoxy-4-methylphenol (Creosol)	0.00	1.72	0.67	1.80	0.72	1.19	1.01	1.13
2-Methoxy-4-vinylphenol (p-vinylguaiacol)	2.08	6.10	2.62	6.31	3.52	0.00	–	–
4-ethyl-2-methoxyphenol	0.00	1.58	0.71	1.81	0.70	1.14	0.29	1.19
2-methoxy-5-(1-propenyl)phenol (Isochavibetol)	0.00	0.38	0.00	1.02	0.39	0.00	–	–
2-methoxy-3-(2-propenyl)phenol (Eugenol)	0.37	0.42	–	–	0.49	0.00	0.42	0.27
4-hydroxy-3-methoxybenzaldehyde (Vanillin)	3.16	1.36	–	–	2.34	0.00	–	–
2-methoxy-4-(1-propenyl)phenol (Isoeugenol)	4.29	3.34	3.76	1.51	4.79	1.40	4.21	1.95
1-(4-hydroxy-3-methoxyphenyl)ethanone (Apocynin)	0.00	1.52	0.00	1.05	1.61	0.00	–	–
1-(4-hydroxy-3-methoxyphenyl)propan-2-one (Guaiacylacetone)	5.11	4.08	3.82	0.00	5.38	0.00	4.00	2.19
3-(4-hydroxy-3-methoxyphenyl)prop-2-enal (Ferulaldehyde)	9.69	1.01	3.11	0.53	1.93	0.00	3.43	0.00
3-(5-formyl-2-hydroxy-3-methoxyphenyl)− 4-hydroxy-5-methoxybenzaldehyde (Divanillin)	–	–	1.18	0.00	–	–	–	–
Sub-total	24.70	23.36	16.70	16.23	22.94	5.27	14.57	8.17
Syringol units (S)								
2,6-dimethoxyphenol (Syringol)	7.83	4.87	4.89	4.07	6.55	5.53	7.85	10.31
2,6-dimethoxy-4-(2-propenyl)phenol (Methoxyeugenol)	7.72	0.98	5.84	2.42	6.69	1.30	8.34	5.20
4-Hydroxy-3,5-dimethoxybenzaldehyde (Syringaldehyde)	3.72	1.34	3.51	1.87	3.16	0.00	4.03	1.13
2,6-dimethoxy-4-[(*Z*)-prop-1-enyl]phenol	1.10	0.22	2.62	1.39	1.45	0.23	1.77	0.70
2,6-dimethoxy-4-[(*E*)-prop-1-enyl]phenol)	0.75	0.19	2.20	1.77	1.08	0.17	1.44	0.67
1-(4-hydroxy-3,5-dimethoxyphenyl)ethanone (Acetosyringone)	1.45	2.27	3.81	3.73	3.45	0.00	3.32	1.60
2-(4-hydroxy-3,5-dimethoxyphenyl)acetic acid	7.88	4.61	7.42	1.86	7.00	1.28	9.49	5.83
3,5-Dimethoxy-4-hydroxycinnamaldehyde (Sinapaldehyde)	7.16	0.62	6.83	0.77	1.82	0.00	8.13	0.65
Sub-total	37.61	15.10	37.12	17.88	31.20	8.51	44.37	26.09
Other lignin derivates compounds (L)								
4-methoxy-3-(methoxymethyl)phenol	2.57	4.51	3.11	2.32	2.72	3.49	2.96	5.99
1-(2,3,4-trihydroxyphenyl)ethanone (Gallacetophenone)	–	0.00	0.41	–	–	–	–	–
1,2,3-trimethoxy-5-methylbenzene	1.60	3.91	2.77	3.08	0.00	2.42	2.12	4.76
1-(3,5-dimethoxyphenyl)ethanone	5.62	5.36	6.76	3.35	6.25	2.67	7.83	7.84
1,2-Dimethoxy-4-(2-methoxyethenyl)benzene	–	0.00	0.30	–	–	–	–	–

(*continued on next page*)

Table 7 (*continued*)

Compound name	L. leucocephala		C. proliferus		P. alba		S. sesban	
	300 °C	365 °C	300 °C	365 °C	325 °C	360 °C	305 °C	360 °C
(E)− 3-(2-methoxy-5-methylphenyl)prop-2-enoic acid	0.00	0.25	0.00	0.82	–	–	0.42	0.00
5-tert-butylbenzene-1,2,3-triol	–	–	1.08	0.00	–	–	–	–
Methyl 2-(3,4-dimethoxyphenyl)− 2-hydroxyacetate	–	5.13	0.00	–	–	–	–	–
Sub-total	9.79	14.03	18.85	10.28	8.97	8.58	13.33	18.59
Other cyclic and aromatics compounds								
1,4:3,6-Dianhydro-D-mannitol	3.20	0.00	–	–	1.57	0.00	2.08	0.00
2,3-dihydro-1,4-dioxine	–	–	3.73	0.00	–	–	–	–
1-(2-methylidenecyclopropyl)ethanone	–	–	–	0.00	1.04	–	–	–
Toluene	–	–	–	–	0.00	4.85	–	–
Phenol	–	–	0.00	1.85	–	–	–	–
3,3,5-trimethyl-2 H-pyran-6-one	–	0.00	0.25	–	–	–	–	–
2-cyclohexyl 2-ethylbutanoate	–	0.00	4.78	–	–	–	–	–
2,6,6-trimethylcyclohexene-1-carbaldehyde	0.00	0.44	–	–	–	–	–	–
4-propylcyclopent-4-ene-1,3-dione	–	0.00	0.33	–	–	–	–	–
9-oxabicyclo[3.3.1]nonan-2-yl acetate	0.00	0.69	–	–	–	–	–	–
3-methylcyclopentane-1,2-dione	–	–	–	0.55	0.00	0.00	1.03	–
Sub-total	3.20	0.69	3.73	7.65	2.12	5.89	2.08	1.03
Other heavy compounds								
Cyclohepta-1,3,5-triene	0.00	0.52	–	–	–	–	–	–
[6-acetyloxy-7-methyl-5-(2-oxopropoxy)− 1,3-dioxepan-4-yl]methyl acetate	0.00	4.09	–	–	8.80	4.10	0.38	3.46
Dimethyl (2E,4E)− 3,4-diethylhexa-2,4-dienedioate	–	–	–	–	0.00	0.69	–	–
3-(1-hydroxy-2-methylprop-2-enyl)− 2,4,4-trimethylcyclohex-2-en-1-one	–	–	0.00	1.69	–	–	–	–
Methyl hexadecanoate (methyl palmitate)	0.46	0.00	–	–	0.00	0.21	0.14	0.12
L-(+)-Ascorbic acid	0.62	0.00	0.24	0.24	1.03	0.00	–	–
L-(+)-Ascorbic acid 2,6-dihexadecanoate	–	–	–	–	–	0.48	0.10	–
Ethyl 1,1-dimethyl-2,3-dihydroindene-4-carboxylate	0.00	0.34	–	–	–	–	–	–
3-hydroxy-3,4-bis[(4-hydroxy-3-methoxyphenyl)methyl]oxolan-2-one ((-)-Nortrachelogenin)	0.00	1.06	–	–	–	–	–	–
10-hydroxy-1,2,3-trimethoxy-6,7-dihydro-5 H-benzo[a]heptalen-9-one	–	–	1.57	0.00	–	–	–	–
Heptacosan-1-ol	–	–	0.36	0.29	–	–	–	–
2,3-dimethoxy-5,6-dihydrobenzo[b][1]benzoxepin-6-ol	0.00	1.75	0.83	0.00	–	–	0.13	0.00
Tetracosan-1-ol	–	–	0.22	0.00	–	–	–	–
Sub-total	1.08	7.42	3.22	2.56	9.83	4.31	1.13	4.37

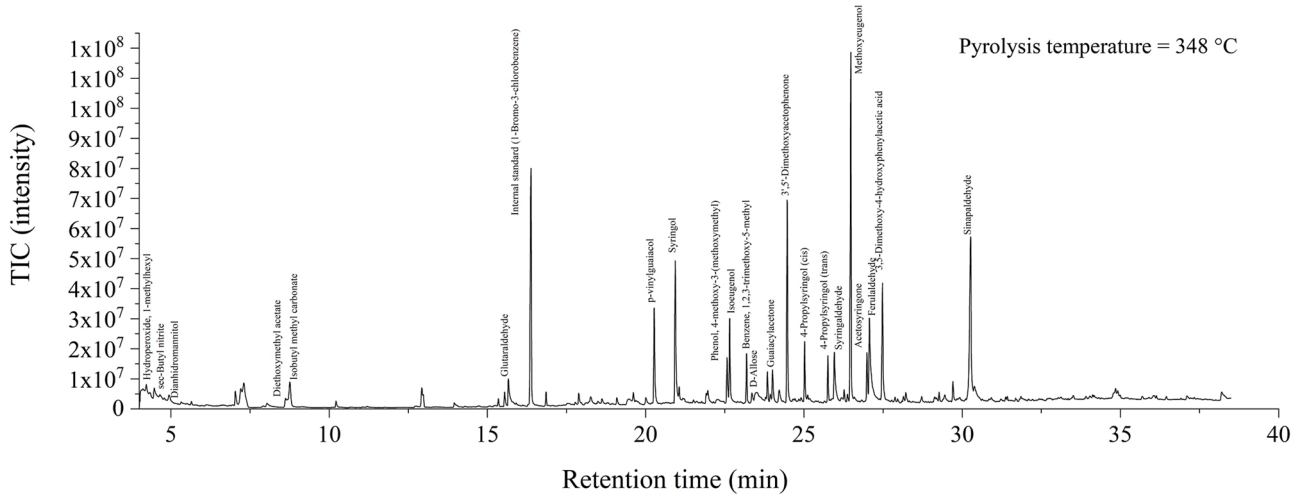

Fig. 4. Representative pyrogram of S. sesban.

L. leucocephala has the lowest concentration among the species with only 5.1% standing out 1,4:3,6-dianhydro-α-D-glucopyranose and 2,3-anhydro-D-galactosan. In particular, the yields of polysaccharides produced by *S. sesban,* and *P. alba* were significantly higher than those of other species of leguminous plants. The initial thermal decomposition of cellulose is the depolymerization of polymers to form various anhydrosugars derivates, among which levoglucosan is the most prevalent and is affected by the cellulose source and condition [62]. The high levoglucosan content (1,6-anhydro-β-D-glucopyranose) of *S. sesban* and *P. alba* is the result of a very rich composition in C_6 sugars and its degradation [63], which agrees with the results of Table 1. With respect to the high D-allose and 3.4-altrosan contents in *C. proliferus*. *S. sesban* and above all *P. alba*, comment that its are typical products obtained from the decomposition of mannan component in the biomass [64], which is part of the C_6 sugars, high content of this type of sugars in *S. sesban* and *P. alba* explains this fact. As it can be observed, wood such as *P. alba* are good candidates to produce interest yields of saccharides with high added value such as D-allose.

Finally, in the case of derivatives of the lignin fraction, a clear downward trend was observed in comparison with the peak of hemicelluloses. The heavier compounds in G, S and L units clearly break down to lighter phenolic products such as guaiacol, syringol, *p*-vinylguaiacol, methoxyeugenol or gallacetophenone. The variety of compounds derived of lignins in the case of *L. leucocephala* and *C. proliferus* is higher compared to the other species owing to the susceptibility to secondary reactions of less compact wood and the shrubby structure of

C. proliferus. It is also observed that the total concentration of these compounds is reduced in all leguminous species but in a very ostensible way in the case of *P. alba*, going from a total of 63.11–22.36% in the cellulose degradation peak. the others only reduced their presence by approximately 20%. The extensive breakdown of C_6 sugars and the hardwood characteristic of *P. alba* making the lignin structure look less attacked at this point might be the cause.

4. Conclusions

In this research, the kinetic characteristics of different species of leguminous pyrolysis process were identified by thermogravimetric analysis experiments coupled with isoconversional method of Kissinger-Akahira-Sunose. Three stages of degradation of biomass during pyrolysis are distinguished: stage I, $\alpha = 0.15–0.35$, decomposition extractives and hemicellulose; stage II, $\alpha = 0.35–0.55$, cellulose and lignin reaction zone; and stage III, $\alpha = 0.55–0.90$, representing the degradation of lignin and minerals. The reaction mechanisms in pyrolysis process have not been completely but, although the degradations of different components interact with each other, certain reaction zones can be appreciated. What is more, by means of the obtained activation energies, diverse thermodynamic parameters such as pre-exponential factor (A), the changes enthalpy (ΔH), free Gibbs energy (ΔG), and entropy (ΔS) have been calculated and discussed, contrasting the complexity of the leguminous pyrolysis process. The enthalpy changes and lower activation energies show that leguminous as *L. leucocephala* or *C. proliferus* require less energy to react in contrast to woodier biomass such as *P. alba* or *S. sesban* that include a high amount of lignins in their composition, making the first two more suitable energetically in thermochemical treatments as pyrolysis.

Strong relationships between volatile compounds detected by Py-GC/MS method and their biomass composition have been established. Operating at low heating rates which it appears that secondary reactions are limited due to their low instability. Therefore, the reaction mechanisms between the volatile products and their components in each biomass can be well observed. The yields of the different products are consistent with the composition of every one of leguminous biomass even at each point of maximum degradation (hemicellulose and cellulose). All biomasses have the potential to produce a wide range of compounds assimilable to bio-oils, however, the amount of levoglucosan and D-allose in the pyrolysis of *P. alba* make this a potentially interesting leguminous.

CRediT authorship contribution statement

Clemente-Castro: Conceptualization, Methodology, Investigation, Formal analysis, Data curation, Visualization. **A. Palma:** Conceptualization, Methodology, Investigation, Formal analysis, Data curation, Visualization, Writing – original draft, Supervision. **M. Ruíz-Montoya:** Conceptualization, Investigation, Formal analysis, Funding adquisition, Supervision, Writing – review & editing. **I. Giráldez:** Methodology, Investigation, Data curation, Funding acquisition, Supervision, Writing – review & editing. **M.J. Díaz:** Conceptualization, Methodology, Investigation, Funding acquisition, Supervision, Writing – review & editing, Project administration.

Declaration of Competing Interest

The authors declare that they have no known competing financial interests or personal relationships that could have appeared to influence the work reported in this paper.

Acknowledgements

This study received financial support from Ministry of Economy and Competitiveness (Spain). National Programme for Research Aimed at the Challenges of Society, CTQ2017-85251-C2-1-R. and the Regional Ministry of Innovation, Science and Enterprise, Government of the Junta de Andalucía (Spain). Operational Programme FEDER Andalusia 2014-2020, Project UHU-1255540. Funding for open access charge: Universidad de Huelva / CBUA.

References

[1] D. Schimel, B.B. Stephens, J.B. Fisher, Effect of increasing CO_2 on the terrestrial carbon cycle, Proc. Natl. Acad. Sci. U. S. A. 112 (2015) 436–441, https://doi.org/10.1073/pnas.1407302112.
[2] H.J. Huang, X.Z. Yuan, Recent progress in the direct liquefaction of typical biomass, Prog. Energy Combust. Sci. 49 (2015) 59–80, https://doi.org/10.1016/j.pecs.2015.01.003.
[3] V. Menon, M. Rao, Trends in bioconversion of lignocellulose: biofuels, platform chemicals & biorefinery concept, Prog. Energy Combust. Sci. 38 (2012) 522–550, https://doi.org/10.1016/j.pecs.2012.02.002.
[4] J.J. Cheng, G.R. Timilsina, Status and barriers of advanced biofuel technologies: a review, Renew, Energy 36 (2011) 3541–3549, https://doi.org/10.1016/j.renene.2011.04.031.
[5] Z. Anwar, M. Gulfraz, M. Irshad, Agro-industrial lignocellulosic biomass a key to unlock the future bio-energy: a brief review, J. Radiat. Res. Appl. Sci. 7 (2014) 163–173, https://doi.org/10.1016/j.jrras.2014.02.003.
[6] S. Zhao, Y. Luo, Multiscale modeling of lignocellulosic biomass thermochemical conversion technology: an overview on the state-of-the-art, Energy Fuels. 34 (2020) 11867–11886, https://doi.org/10.1021/acs.energyfuels.0c02247.
[7] M.N. Uddin, K. Techato, J. Taweekun, M.M. Rahman, M.G. Rasul, T.M.I. Mahlia, S. M. Ashrafur, An overview of recent developments in biomass pyrolysis technologies, Energies 11 (2018), https://doi.org/10.3390/en11113115.
[8] R. Wochesländer, R.J. Harper, S.R. Sochacki, P.R. Ward, C. Revell, Tagasaste (Cytisus proliferus Link.) reforestation as an option for carbon mitigation in dryland farming systems, Ecol. Eng. 97 (2016) 610–618, https://doi.org/10.1016/j.ecoleng.2016.10.039.
[9] J. Payormhorm, K. Kangvansaichol, P. Reubroycharoen, P. Kuchonthara, N. Hinchiranan, Pt/Al2O3-catalytic deoxygenation for upgrading of Leucaena leucocephala-pyrolysis oil, Bioresour. Technol. 139 (2013) 128–135, https://doi.org/10.1016/j.biortech.2013.04.023.
[10] J.M. Loaiza, F. López, M.T. García, J.C. García, M.J. Díaz, Biomass valorization by using a sequence of acid hydrolysis and pyrolysis processes. application to Leucaena leucocephala, Fuel 203 (2017) 393–402, https://doi.org/10.1016/j.fuel.2017.04.135.
[11] O. Iglesias, R. Rivas, P. García-Fraile, A. Abril, P.F. Mateos, E. Martinez-Molina, E. Velázquez, Genetic characterization of fast-growing rhizobia able to nodulate Prosopis alba in North Spain, FEMS Microbiol. Lett. 277 (2007) 210–216, https://doi.org/10.1111/j.1574-6968.2007.00968.x.
[12] F. Kwesiga, R. Coe, The effect of short rotation Sesbania sesban planted fallows on maize yield, . Ecol. Manag. 64 (1994) 199–208, https://doi.org/10.1016/0378-1127(94)90294-1.
[13] A. Alfaro, F. López, A. Pérez, J.C. García, A. Rodríguez, Integral valorization of tagasaste (Chamaecytisus proliferus) under hydrothermal and pulp processing, Bioresour. Technol. 101 (2010) 7635–7640, https://doi.org/10.1016/j.biortech.2010.04.059.
[14] A. Anca-Couce, C. Tsekos, S. Retschitzegger, F. Zimbardi, A. Funke, S. Banks, T. Kraia, P. Marques, R. Scharler, W. de Jong, N. Kienzl, Biomass pyrolysis TGA assessment with an international round robin, Fuel 276 (2020), 118002, https://doi.org/10.1016/j.fuel.2020.118002.
[15] Z. Ma, D. Chen, J. Gu, B. Bao, Q. Zhang, Determination of pyrolysis characteristics and kinetics of palm kernel shell using TGA-FTIR and model-free integral methods, Energy Convers. Manag. 89 (2015) 251–259, https://doi.org/10.1016/j.enconman.2014.09.074.
[16] L. Luo, X. Guo, Z. Zhang, M. Chai, M.M. Rahman, X. Zhang, J. Cai, Insight into pyrolysis kinetics of lignocellulosic biomass: isoconversional kinetic analysis by the modified friedman method, Energy Fuels. 34 (2020) 4874–4881, https://doi.org/10.1021/acs.energyfuels.0c00275.
[17] J. Cai, D. Xu, Z. Dong, X. Yu, Y. Yang, S.W. Banks, A.V. Bridgwater, Processing thermogravimetric analysis data for isoconversional kinetic analysis of lignocellulosic biomass pyrolysis: Case study of corn stalk, Renew. Sustain. Energy Rev. 82 (2018) 2705–2715, https://doi.org/10.1016/j.rser.2017.09.113.
[18] X. Yang, R. Zhang, J. Fu, S. Geng, J.J. Cheng, Y. Sun, Pyrolysis kinetic and product analysis of different microalgal biomass by distributed activation energy model and pyrolysis-gas chromatography-mass spectrometry, Bioresour. Technol. 163 (2014) 335–342, https://doi.org/10.1016/j.biortech.2014.04.040.
[19] F. Nsaful, F.X. Collard, M. Carrier, J.F. Görgens, J.H. Knoetze, Lignocellulose pyrolysis with condensable volatiles quantification by thermogravimetric analysis - thermal desorption/gas chromatography-mass spectrometry method, J. Anal. Appl. Pyrolysis 116 (2015) 86–95, https://doi.org/10.1016/j.jaap.2015.10.002.
[20] M.Z. Zayed, S.M.A. Sallam, N.D. Shetta, Review article on leucaena leucocephala as one of the miracle timber trees, Int. J. Pharm. Pharm. Sci. 10 (2018) 1, https://doi.org/10.22159/ijpps.2018v10i1.18250.
[21] J. Donate-Correa, M. León-Barrios, R. Pérez-Galdona, Screening for plant growth-promoting rhizobacteria in Chamaecytisus proliferus (tagasaste), a forage tree-shrub legume endemic to the Canary Islands, Plant Soil 2004 2661 (266) (2005) 261–272, https://doi.org/10.1007/S11104-005-0754-5.

[22] A.B. Cisneros, J.G. Moglia, Prosopis alba, alternativa sustentable para zonas áridas y semiáridas, Los Bosques Actuales Del Chaco Semiárido Argentino Ecoanatomia y Biodivers, Una Mirada Posit. (2017) 231–248.
[23] F.R. Kwesiga, S. Franzel, F. Place, D. Phiri, C.P. Simwanza, Sesbania sesban improved fallows in eastern Zambia: their inception, development and farmer enthusiasm, Agrofor. Syst. 1999 47 (471) (1999) 49–66, https://doi.org/10.1023/A:1006256323647.
[24] J. Walkinshaw, P. Properties, Sampl. Prep. wood Anal. (Propos. Revis. T 257 cm-02 a Stand. Pract.) (2012).
[25] K.K. Moisture, Volatile matter, ash, and fixed carbon determination in coke. application note. instrument: TGA801, Reproduction 06 (2008) 2–3.
[26] T-204, Solvent extractives of wood and pulp, Tappi Test. Methods T-204 cm 0 (2007).
[27] T-249, Carbohydrate composition of extractive-free wood and wood pulp by gas-liquid chromatograph, Tappi Test. Methods T 257 cm 8 (1985).
[28] C.M. Guldberg, P. Waage, Ueber die chemische Affinität. § 1. Einleitung, J. Für Prakt. Chem. 19 (1879) 69–114, https://doi.org/10.1002/prac.18790190111.
[29] S. Arrhenius, Über die Reaktionsgeschwindigkeit bei der Inversion von Rohrzucker durch Säuren, Z. Für Phys. Chem. 4U (1889) 226–248, https://doi.org/10.1515/ZPCH-1889-0416.
[30] OzawaTakeo, A N. Method Anal. Thermogravim. Data 38 (2006) 1881–1886, https://doi.org/10.1246/BCSJ.38.1881. Http://Dx.Doi.Org/10.1246/Bcsj.38.1881.
[31] A.W. COATS, J.P. REDFERN, Kinetic Parameters from Thermogravimetric Data, Nat 1964 201 (2014914) (1964) 68–69, https://doi.org/10.1038/201068a0.
[32] A.A.D. Maia, L.C. de Morais, Kinetic parameters of red pepper waste as biomass to solid biofuel, Bioresour. Technol. 204 (2016) 157–163, https://doi.org/10.1016/j.biortech.2015.12.055.
[33] X. Yuan, T. He, H. Cao, Q. Yuan, Cattle manure pyrolysis process: kinetic and thermodynamic analysis with isoconversional methods, Renew. Energy 107 (2017) 489–496, https://doi.org/10.1016/j.renene.2017.02.026.
[34] D. Neves, H. Thunman, A. Matos, L. Tarelho, A. Gómez-Barea, Characterization and prediction of biomass pyrolysis products, Prog. Energy Combust. Sci. 37 (2011) 611–630, https://doi.org/10.1016/j.pecs.2011.01.001.
[35] M. Fodil Cherif, D. Trache, N. Brosse, F. Benaliouche, A.F. Tarchoun, Comparison of the physicochemical properties and thermal stability of organosolv and kraft lignins from hardwood and softwood biomass for their potential valorization, Waste Biomass-.-. Valoriz. 11 (2020) 6541–6553, https://doi.org/10.1007/s12649-020-00955-0.
[36] L. Jiménez, A. Pérez, M.J. de la Torre, A. Moral, L. Serrano, Characterization of vine shoots, cotton stalks, Leucaena leucocephala and Chamaecytisus proliferus, and of their ethyleneglycol pulps, Bioresour. Technol. 98 (2007) 3487–3490, https://doi.org/10.1016/j.biortech.2006.11.009.
[37] M.J. Díaz, R. Yañez, A. García Barneto, J.E. Martín Alfonso, M.J. Feria, R. Tapias, M. Fernández, Variations in production and oligomers content obtained under hydrothermal treatment among five fast-growing species, Open Agric. J. 4 (2014) 87–92, https://doi.org/10.2174/1874331501004010087.
[38] V. Kothiyal, A. Raturi, A. Kaler, S. Naithani, Klason lignin estimation in Leucaena leucocephala by near infrared spectroscopy for selection of superior material for pulp and paper, J. Indian Acad. Wood Sci. 9 (2012) 105–114, https://doi.org/10.1007/s13196-012-0078-z.
[39] B. Hu, W.L. Xie, H. Li, K. Li, Q. Lu, Y.P. Yang, On the mechanism of xylan pyrolysis by combined experimental and computational approaches, Proc. Combust. Inst. 38 (2021) 4215–4223, https://doi.org/10.1016/j.proci.2020.06.172.
[40] L.A. Donaldson, Lignification and lignin topochemistry - an ultrastructural view, Phytochemistry 57 (2001) 859–873, https://doi.org/10.1016/S0031-9422(01)00049-8.
[41] S.S. Kim, A. Shenoy, F.A. Agblevor, Thermogravimetric and kinetic study of Pinyon pine in the various gases, Bioresour. Technol. 156 (2014) 297–302, https://doi.org/10.1016/j.biortech.2014.01.066.
[42] T. Sebio-Puñal, S. Naya, J. López-Beceiro, J. Tarrío-Saavedra, R. Artiaga, Thermogravimetric analysis of wood, holocellulose, and lignin from five wood species, J. Therm. Anal. Calorim. 109 (2012) 1163–1167, https://doi.org/10.1007/s10973-011-2133-1.
[43] Y.C. Lin, J. Cho, G.A. Tompsett, P.R. Westmoreland, G.W. Huber, Kinetics and mechanism of cellulose pyrolysis, J. Phys. Chem. C. 113 (2009) (2009) 7–20107, https://doi.org/10.1021/jp906702p.
[44] P.E. Sánchez-Jiménez, L.A. Pérez-Maqueda, A. Perejón, J.M. Criado, Generalized master plots as a straightforward approach for determining the kinetic model: the case of cellulose pyrolysis, Thermochim. Acta 552 (2013) 54–59, https://doi.org/10.1016/j.tca.2012.11.003.
[45] M.E. SantosMiranda, C. Marcolla, C.A. Rodriguez, H.M. Wilhelm, M. R. Sierakowski, T.M. BelleBresolin, R. Alves de Freitas, I. The role of N-carboxymethylation of chitosan in the thermal stability and dynamic, Polym. Int 55 (2006) 961–969, https://doi.org/10.1002/pi.
[46] B.L.F. Chin, S. Yusup, A. Al Shoaibi, P. Kannan, C. Srinivasakannan, S.A. Sulaiman, Kinetic studies of co-pyrolysis of rubber seed shell with high density polyethylene, Energy Convers. Manag. 87 (2014) 746–753, https://doi.org/10.1016/j.enconman.2014.07.043.
[47] T. Zhang, X. Li, X. Qiao, M. Zheng, L. Guo, W. Song, W. Lin, Initial mechanisms for an overall behavior of lignin pyrolysis through large-scale reaxFF molecular dynamics simulations, Energy Fuels. 30 (2016) 3140–3150, https://doi.org/10.1021/acs.energyfuels.6b00247.
[48] J.Y. Yeo, B.L.F. Chin, J.K. Tan, Y.S. Loh, Comparative studies on the pyrolysis of cellulose, hemicellulose, and lignin based on combined kinetics, J. Energy Inst. 92 (2019) 27–37, https://doi.org/10.1016/j.joei.2017.12.003.
[49] M. Carrier, A. Loppinet-Serani, D. Denux, J.M. Lasnier, F. Ham-Pichavant, F. Cansell, C. Aymonier, Thermogravimetric analysis as a new method to determine the lignocellulosic composition of biomass, Biomass-. Bioenergy 35 (2011) 298–307, https://doi.org/10.1016/j.biombioe.2010.08.067.
[50] C.M. Santos, J. Dweck, R.S. Viotto, A.H. Rosa, L.C. de Morais, Application of orange peel waste in the production of solid biofuels and biosorbents, Bioresour. Technol. 196 (2015) 469–479, https://doi.org/10.1016/j.biortech.2015.07.114.
[51] Y. Xu, B. Chen, Investigation of thermodynamic parameters in the pyrolysis conversion of biomass and manure to biochars using thermogravimetric analysis, Bioresour. Technol. 146 (2013) 485–493, https://doi.org/10.1016/j.biortech.2013.07.086.
[52] S.C. Turmanova, S.D. Genieva, A.S. Dimitrova, L.T. Vlaev, Non-isothermal degradation kinetics of filled with rise husk ash polypropene composites, Express Polym. Lett. 2 (2008) 133–146, https://doi.org/10.3144/expresspolymlett.2008.18.
[53] Y.S. Kim, Y.S. Kim, S.H. Kim, Investigation of thermodynamic parameters in the thermal decomposition of plastic waste-waste lube oil compounds, Environ. Sci. Technol. 44 (2010) 5313–5317, https://doi.org/10.1021/es101163e.
[54] S. Wang, B. Ru, H. Lin, W. Sun, Pyrolysis behaviors of four O-acetyl-preserved hemicelluloses isolated from hardwoods and softwoods, Fuel 150 (2015) 243–251, https://doi.org/10.1016/j.fuel.2015.02.045.
[55] S. Deng, Y.P. Ting, Characterization of PEI-modified biomass and biosorption of Cu (II), Pb(II) and Ni(II), Water Res 39 (2005) 2167–2177, https://doi.org/10.1016/j.watres.2005.03.033.
[56] Y. Luo, Z. Li, X. Li, X. Liu, J. Fan, J.H. Clark, C. Hu, The production of furfural directly from hemicellulose in lignocellulosic biomass: a review, Catal. Today 319 (2019) 14–24, https://doi.org/10.1016/j.cattod.2018.06.042.
[57] T. Hosoya, H. Kawamoto, S. Saka, Secondary reactions of lignin-derived primary tar components, J. Anal. Appl. Pyrolysis 83 (2008) 78–87, https://doi.org/10.1016/j.jaap.2008.06.003.
[58] D.R. Naron, F.X. Collard, L. Tyhoda, J.F. Görgens, Characterisation of lignins from different sources by appropriate analytical methods: introducing thermogravimetric analysis-thermal desorption-gas chromatography–mass spectroscopy, Ind. Crops Prod. 101 (2017) 61–74, https://doi.org/10.1016/j.indcrop.2017.02.041.
[59] S. Wang, B. Ru, G. Dai, H. Lin, L. Zhang, Influence mechanism of torrefaction on softwood pyrolysis based on structural analysis and kinetic modeling, Int. J. Hydrog. Energy 41 (2016) 16428–16435, https://doi.org/10.1016/j.ijhydene.2016.02.082.
[60] Q. Lu, W.M. Xiong, W.Z. Li, Q.X. Guo, X.F. Zhu, Catalytic pyrolysis of cellulose with sulfated metal oxides: a promising method for obtaining high yield of light furan compounds, Bioresour. Technol. 100 (2009) 4871–4876, https://doi.org/10.1016/j.biortech.2009.04.068.
[61] F.X. Collard, J. Blin, A review on pyrolysis of biomass constituents: mechanisms and composition of the products obtained from the conversion of cellulose, hemicelluloses and lignin, Renew. Sustain. Energy Rev. 38 (2014) 594–608, https://doi.org/10.1016/j.rser.2014.06.013.
[62] D.K. Shen, S. Gu, The mechanism for thermal decomposition of cellulose and its main products, Bioresour. Technol. 100 (2009) 6496–6504, https://doi.org/10.1016/j.biortech.2009.06.095.
[63] J. Li, X. Bai, Y. Fang, Y. Chen, X. Wang, H. Chen, H. Yang, Comprehensive mechanism of initial stage for lignin pyrolysis, Combust. Flame. 215 (2020) 1–9, https://doi.org/10.1016/j.combustflame.2020.01.016.
[64] T.A. Ngo, J. Kim, S.S. Kim, Fast pyrolysis of palm kernel cake using a fluidized bed reactor: Design of experiment and characteristics of bio-oil, J. Ind. Eng. Chem. 19 (2013) 137–143, https://doi.org/10.1016/j.jiec.2012.07.015.